Program Digest, 2019 IEEE International Ultrasonics Symposium (IUS)
Glasgow, Scotland, October 6-9, 2019

Agent-Free Super-Resolution High-Speed Photoacoustic Microscopy

Jongbeom Kim
Departments of Creative IT Engineering
Pohang University of Science and Technology (POSTECH)
Pohang, Republic of Korea
worrma@postech.ac.kr

Jin Young Kim
Departments of Creative IT Engineering
Pohang University of Science and Technology (POSTECH)
Pohang, Republic of Korea
ronsan@postech.ackr

Seungwan Jeon
Departments of Creative IT Engineering
Pohang University of Science and Technology (POSTECH)
Pohang, Republic of Korea
jsw777@postech.ac.kr

Jin Woo BAIK
Departments of Creative IT Engineering
Pohang University of Science and Technology (POSTECH)
Pohang, Republic of Korea
bjwpp12@postech.ac.kr

Seong Hee Cho
School of Interdisciplinary Bioscience and Bioengineering
Pohang University of Science and Technology (POSTECH)
Pohang, Republic of Korea
shcho89@postech.ac.kr

Chulhong Kime
Departments of Creative IT Engineering
Pohang University of Science and Technology (POSTECH)
Pohang, Republic of Korea
chulhong@postech.edu

***Abstract*—Photoacoustic microscopy (PAM) based on the photoacoustic (PA) effect showed the ability of anatomical, functional, metabolic and pathological imaging of animals and humans *in vivo*. However, the developed PAM systems have not achieved a fast temporal resolution and a high spatial resolution due to physical constraints. To overcome this, microelectromechanical systems (MEMS) scanners have been used for fast scanning speed and super-resolution technologies have been applied for the high spatial resolution. However, the MEMS scanners have shown unstable scanning patterns, and the super-resolution methods have slowed down imaging and required an external contrast agent. Here, we report an agent-free super-resolution high-speed PAM based on a fast scanner (AF-SR-PAM) that overcomes both the spatial and temporal resolution limitations. The scanner was used to steer the optical beam and acoustic wave together, achieving a high signal-to-noise ratio and a B-mode image rate of 500 Hz. Furthermore, by applying our super-resolution method, unresolved micro-vessels in a conventional PAM system are separated in the PA images of AF-SR-PAM. This improvement enables the observation of microvasculature in animals *in vivo*.**

Keywords—photoacoustic microscopy, fast imaging

I. Introduction

Photoacoustic microscopy (PAM) based on a photoacoustic (PA) effect is a promising biomedical microscope capable of non-invasive imaging [1]. The PA effect is a phenomenon that a sound wave occurs when molecules undergo thermal expansion due to the instantaneous absorption of light. Photoacoustic microscopy uses a ultrasound transducer to measure ultrasound waves from tissues excited by a nanosecond pulsed laser beam. PAM, which uses the target's absorption of light, has a richer light absorption contrast than conventional optical microscopy techniques. With these features, PAM analyzes anatomical and functional information of animals and humans *in vivo* in various fields of research, such as biology, oncology, neurology, ophthalmology and pathology [1-13]. However, the conventional PAM system using a linear motorized stage has a disadvantage of slow imaging speed. In addition, conventional super-resolution PA imaging techniques that achieve high spatial resolution have the disadvantage of slowing the imaging speed or using an exogenous contrast agent.

Many studies have been conducted to achieve fast temporal and high spatial resolutions. The imaging speed is technically dependent on the laser pulse repetition rate (PRR) and the scanning mechanism. Fast laser systems have already been developed to reach the theoretical marginal imaging speed [14]. Although the scanning mechanism has not reached the conditions for the maximum imaging speed, the use of microelectromechanical systems (MEMS) scanners, a hexagon-mirror and galvanometer scanners has improved the imaging speed [13, 15, 16]. The MEMS scanner, however, showed unstable scanning patterns, and the hexagon mirror had a wide step size with a fixed scanning range. The galvanometer scanner failed to confocally steer optical beams and acoustic waves, resulting in a low signal-to-noise ratio or a narrow wide field of view (FOV) [17, 18].

Non-linear PA effects using the photo bleaching or light saturation methods in PAM achieved super resolution [19, 20]. However, the short working distance due to the large optical NA prevented the use of other scanners, which slowed down the imaging. Although high spatial resolution was also achieved using localization techniques in PAI, ultrasound imaging, and fluorescence microscopy, clinically undesirable exogenous contrast agents such as microspheres or microbubbles had to be used in these methods [21-24].

Here we report an agent-free super-resolution high-speed PAM based a scanner (AF-SR-PAM). The scanner steers both

laser beams and acoustic waves quickly to achieve high SNR while maintaining fast scan rates. This fast scanning and high SNR enable to apply our super-resolution method. The B-scan rate was increased to 500 Hz and the micro-vessels that were unresolved in conventional PAM were separated by AF-SR-PAM. Based on these improvements, we observed *in vivo* microvascular anatomy in small animals..

II. Method

A. *Agent-free super-resolution high-speed photoacoustic microscopy*

First, the trigger signal for a laser system (VPFL-G-10, Spectra-Physics, USA) was generated by a multifunction data acquisition board (DAQ, NI PCIe-6321, National Instruments, USA). To generate a PA signal, we used the pulse laser of 532 nm wavelength. The generated PA wave was detected by an ultrasonic transducer (v214-BC-RM, 50-MHz center frequency, Olympus NDT, USA) and converted it into an electrical signal. We also used the DAQ board to synchronize the laser system, a high-speed scanner and a motorized stage (L-406, UK Physik instrumente LTD). Fast scanner movement provides B mode images. At the same time, the object was moved by the motorized stage to create a volume image.

III. Result and Discussion

Figure 1 displays a schematic of the AF-SR-PAM system. We accomplished fast vascular imaging with the scanner and the pulsed laser system with an optical wavelength of 532 nm and a PRR of 800 kHz. We also used the scanner to quickly scan the generated laser pulses. In particular, the scanner's mirror was immersed in water to handle both the optical beam and the PA wave. AF-SR-PAM ensures stable scanning up to a B-scan rate of 500 Hz underwater. The scanner has a scanning range of up to 2.4 mm and the motorized stage has a scanning range of up to 26 mm. The SNR was maximized using an opto-acoustic combiner that coaxially and confocally align the optical beam and the generated PA wave. The SNR in the PA image of mouse ears *in vivo* is 35.6 dB. Prior to *in vivo* experiments, we conducted a phantom experiment that photoacoustically imaged a microstructure pattern and a microfiber to measure spatial resolutions. The lateral resolution was measured by imaging the microstructure pattern. The measured lateral resolution was 7.5 μm. In addition, the axial resolution measured by imaging the microfiber was 33.0 μm.

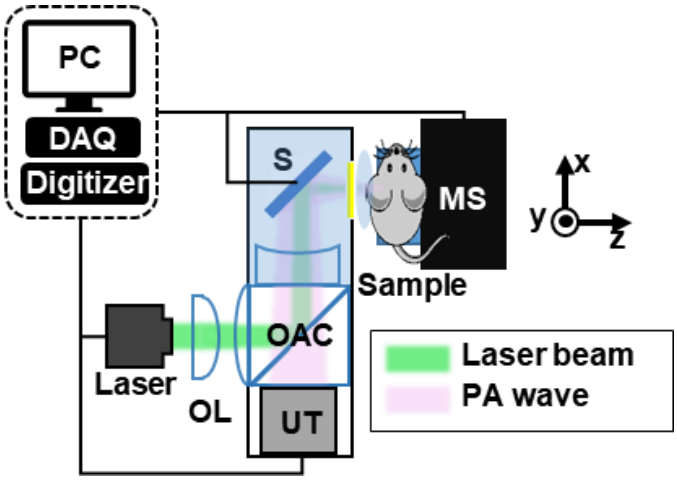

Fig. 1. Schematic of AF-SR-PAM. OL, objective lens; UT, ultrasound transducer; OAC, opto-acoustic combiner; S, scanner; MS, motorized stage.

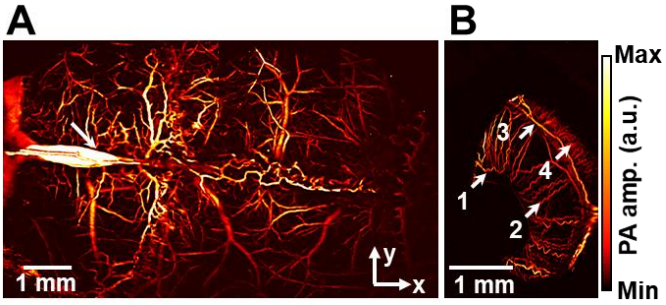

Fig. 2. A. Wide FOV PA MAP image of the mouse brain. Superior sagittal sinus is highlighted by the white arrow. B. PA MAP image of the mouse eye. Circulus arteriosus major (1), iris (2), circulus arteriosus minor (3) and choroid blood vessels (4) are highlighted by the white arrows, respectively.

We conducted *in vivo* experiments that imaged the brain and eye of the mouse. First, we got a microvasculature image of the mouse's brain (Fig. 2A). The images of the entire brain are composed of four segmented images. The size of each segmented image is 2.4 mm × 6 mm (x and y axes, respectively). It took 2.4 s to obtain one segmented image. The superior sagittal sinus is observed and is highlighted by a white arrow. Next we photoacoustically imaged the mouse eye (Fig. 2B). The size of the mouse eye image is 2.4 mm × 4 mm and it took 0.8 s to obtain it. The PA MAP image clearly displays the anatomy of the eye such as circulus arteriosus major, iris, circulus arteriosus minor and choroid blood vessels. Furthermore, we applied the agent-free super-resolution technique to resolve blood vessels that do not resolve in the regular PA image.

IV. Conclusion

We achieved a fast B-mode imaging speed using the scanner and the fast laser system. To maximize SNR, the laser beam and acoustic wave are steered by the scanner underwater while maintaining coaxial and confocal alignment. Using this fast imaging speed, we photoacoustically imaged the brain and eye of the mouse. PA MAP images taken by AF-SR-PAM showed the major anatomical micro-vessels. Furthermore, the spatial resolution is improved by applying an agent-free super-resolution method. AF-SR-PAM has great potential in various fields such as neurology, oncology and pathology.

Acknowledgment *(Heading 5)*

This work was supported by the National Research Foundation of Korea(NRF) grant funded by the Korea government(MSIT) (No. NRF-2019R1A2C2006269).

※ MSIT : Ministry of Science and ICT

REFERENCES

[1] J. Yao and L. V. Wang, "Photoacoustic microscopy," *Laser & photonics reviews,* vol. 7, no. 5, pp. 758-778, 2013.

[2] S. Jeon *et al.*, "In vivo photoacoustic imaging of anterior ocular vasculature: a random sample consensus approach," *Scientific Reports,* vol. 7, no. 1, p. 4318, 2017.

[3] S. Jeon, J. Park, R. Managuli, and C. Kim, "A Novel 2D Synthetic Aperture Focusing Technique for Acoustic-resolution Photoacoustic Microscopy," *IEEE transactions on medical imaging,* 2018.

[4] B. Park, H. Lee, S. Jeon, J. Ahn, H. H. Kim, and C. Kim, "Reflection-mode switchable subwavelength Bessel-beam and Gaussian-beam photoacoustic microscopy in vivo," *Journal of biophotonics,* p. e201800215, 2018.

[5] B. Park, H. Lee, P. K. Upputuri, M. Pramanik, D. Kim, and C. Kim, "Super-resolution photoacoustic microscopy using near-field localization by a plasmonic metal nanoaperture: a simulation study," *IEEE Journal of Selected Topics in Quantum Electronics,* vol. 25, no. 2, pp. 1-7, 2019.

[6] D. Lee *et al.*, "In Vivo Photoacoustic Imaging of Livers Using Biodegradable Hyaluronic Acid-Conjugated Silica Nanoparticles," *Advanced Functional Materials,* vol. 28, no. 22, p. 1800941, 2018.

[7] K. Park, J. Y. Kim, C. Lee, S. Jeon, G. Lim, and C. Kim, "Handheld Photoacoustic Microscopy Probe," *Scientific reports,* vol. 7, no. 1, p. 13359, 2017.

[8] D. Lee, C. Lee, S. Kim, Q. Zhou, J. Kim, and C. Kim, "In vivo near infrared virtual intraoperative surgical photoacoustic optical coherence tomography," *Scientific reports,* vol. 6, p. 35176, 2016.

[9] J. Kim, D. Lee, U. Jung, and C. Kim, "Photoacoustic imaging platforms for multimodal imaging," *Ultrasonography,* vol. 34, no. 2, p. 88, 2015.

[10] S. Jeon, J. Kim, D. Lee, B. J. Woo, and C. J. P. Kim, "Review on practical photoacoustic microscopy," p. 100141, 2019.

[11] J. Kim *et al.*, "Real-time Photoacoustic Thermometry Combined with Clinical Ultrasound Imaging and High Intensity Focused Ultrasound," 2019.

[12] J. Y. Kim, C. Lee, K. Park, S. Han, and C. Kim, "High-speed and high-SNR photoacoustic microscopy based on a galvanometer mirror in non-conducting liquid," *Scientific reports,* vol. 6, p. 34803, 2016.

[13] J. Y. Kim, C. Lee, K. Park, G. Lim, and C. Kim, "Fast optical-resolution photoacoustic microscopy using a 2-axis water-proofing MEMS scanner," *Scientific reports,* vol. 5, p. 7932, 2015.

[14] Y. Liang, L. Jin, B.-O. Guan, and L. Wang, "2 MHz multi-wavelength pulsed laser for functional photoacoustic microscopy," *Optics letters,* vol. 42, no. 7, pp. 1452-1455, 2017.

[15] J. Yao *et al.*, "Wide-field fast-scanning photoacoustic microscopy based on a water-immersible MEMS scanning mirror," *Journal of biomedical optics,* vol. 17, no. 8, p. 080505, 2012.

[16] B. Lan *et al.*, "High-speed widefield photoacoustic microscopy of small-animal hemodynamics," *Biomedical optics express,* vol. 9, no. 10, pp. 4689-4701, 2018.

[17] B. Rao, L. Li, K. Maslov, and L. Wang, "Hybrid-scanning optical-resolution photoacoustic microscopy for in vivo vasculature imaging," *Optics letters,* vol. 35, no. 10, pp. 1521-1523, 2010.

[18] P. Hajireza, W. Shi, and R. Zemp, "Label-free in vivo fiber-based optical-resolution photoacoustic microscopy," *Optics letters,* vol. 36, no. 20, pp. 4107-4109, 2011.

[19] J. Yao, L. Wang, C. Li, C. Zhang, and L. V. Wang, "Photoimprint photoacoustic microscopy for three-dimensional label-free subdiffraction imaging," *Physical review letters,* vol. 112, no. 1, p. 014302, 2014.

[20] A. Danielli *et al.*, "Label-free photoacoustic nanoscopy," *Journal of biomedical optics,* vol. 19, no. 8, p. 086006, 2014.

[21] X. L. Dean-Ben and D. Razansky, "Localization optoacoustic tomography," *Light: Science & Applications,* vol. 7, no. 4, p. 18004, 2018.

[22] C. Errico *et al.*, "Ultrafast ultrasound localization microscopy for deep super-resolution vascular imaging," *Nature,* vol. 527, no. 7579, p. 499, 2015.

[23] B. Huang, M. Bates, and X. Zhuang, "Super-resolution fluorescence microscopy," *Annual review of biochemistry,* vol. 78, pp. 993-1016, 2009.

[24] W. Choi and C. Kim, "Toward in vivo translation of super-resolution localization photoacoustic computed tomography using liquid-state dyed droplets," 2019.